EurJIC
European Journal of Inorganic Chemistry

Full Paper
doi.org/10.1002/ejic.202000835

Alkyne Metathesis

Synthesis of Alkyne Metathesis Catalysts from Tris(dimethylamido)tungsten Precursors

Daniel Melcher,[a] Òscar Àrias,[a] Matthias Freytag,[a] Peter G. Jones,[a] and Matthias Tamm*[a]

Dedicated to Professor Richard R. Schrock on the occasion of his 75th birthday

Abstract: Benzylidyne tungsten systems bearing a combination of alkoxide and amide ligands were readily obtained by partial alcoholysis of amido-supported tungsten complexes. Benzylidyne tris(dimethylamido)tungsten was treated with fluorinated alcohols $Me_2(CF_3)COH$, $Me(CF_3)_2COH$, and $(CF_3)_3COH$, and also with silanols $(tBuO)_3SiOH$, and Ph_3SiOH, all of which resulted in complexes of the type $[PhC{\equiv}W(NHMe_2)(NMe_2)(OR)_2]$. Full displacement of the amido ligands was also achieved in $[PhC{\equiv}W(NHMe_2)\{OC(CF_3)_2Me\}\{OSi(O\text{-}tBu)_3\}_2]$ and $[PhC{\equiv}W(NHMe_2)(OSiPh_3)_3]$. In addition, reaction of the three fluorinated alcohols with hexakis(dimethylamido)ditungsten yielded isomeric mixtures of bimetallic complexes $[W_2(NMe_2)_4(OR)_2]$, which bear two electron-donating ligands and one electron-withdrawing ligand per tungsten atom. All amido-substituted compounds are active in the self-metathesis of 5-benzyloxy-2-pentyne, although $[W_2(OR)_2(NMe_2)_4]$ complexes require longer initiation times depending on the degree of fluorination of the *tert*-butoxide ligand.

Introduction

Alkyne metathesis, discovered half a century ago,[1] has for a long time remained in the shadow of the much more familiar olefin metathesis. Its potential, however, has become clear with the development of suitable synthetic approaches to tungsten and molybdenum alkylidyne complexes.[2] Especially for tungsten, three main precursors can be highlighted (Scheme 1). Precursor $[Me_3CC{\equiv}W(Cl)_3(dme)]$ (**1**; dme = 1,2-dimethoxyethane) was prepared by Schrock et al. via the "high-oxidation-state" route,[3] and gave access to a long series of tungsten alkylidyne complexes bearing a variety of alkoxide ligands. Starting from WCl_6, versatile complex **1** is obtained in three steps, and can be reacted further via salt metathesis to generate different tungsten alkylidyne complexes. A major drawback is the lack of variability in the alkylidyne fragment, which may however subsequently be exchanged by cross-metathesis with alkynes.[4] This disadvantage is overcome in the "low-oxidation-state" route. Thereby, addition of lithium salts to metal carbonyls forms Fischer-type carbene complexes, which may be further oxidized to give $[ArC{\equiv}W(Br)_3(dme)]$ (**2**; Ar = aryl).[5]

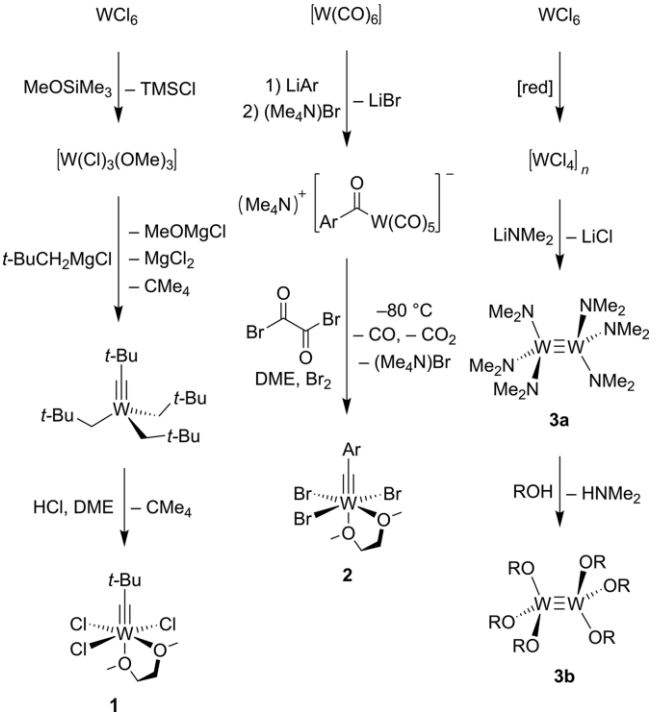

Scheme 1. Selected precursors for the synthesis of tungsten alkylidyne complexes. Abbreviations: Ar, aryl; DME, 1,2-dimethoxyethane; R, alkyl chain; red, reductant (preferably Sn); TMS, trimethylsilyl.

The third method, the ditungsten route,[6] has received less attention than the other two and is based on dinuclear precursors $[W_2(NMe_2)_6]$ (**3a**) and $[W_2(OR)_6]$ (**3b**). Synthesis of **3a** is achieved by salt metathesis of WCl_4 with $LiNMe_2$.[7] WCl_4 can be synthesized from WCl_6 via reduction with tin.[8] In contrast

[a] *Dr. D. Melcher, Dr. Ò. Àrias, Dr. M. Freytag, Prof. Dr. P. G. Jones, Prof. Dr. M. Tamm*
Institut für Anorganische und Analytische Chemie, Technische Universität Braunschweig,
Hagenring 30, 38106 Braunschweig, Germany
E-mail: m.tamm@tu-braunschweig.de
https://www.tu-braunschweig.de/iaac/personal/prof-dr-m-tamm
Supporting information and ORCID(s) from the author(s) for this article are available on the WWW under https://doi.org/10.1002/ejic.202000835.

Full Paper
doi.org/10.1002/ejic.202000835

to the high- and low-oxidation-state routes, the amido ligands are exchanged simply by alcoholysis to generate **3b**, a reaction that was intensively studied by Chisholm.[8b,9] In particular, the fluorinated derivative $[W_2(OC(CF_3)Me_2)_6]$[6h] was recently reported to be highly efficient in the metathesis of internal and terminal alkynes. An alternative route to **3b** was developed by Schrock,[6a] who investigated the metathesis reactions of these ditungsten complexes with alkynes, during which the tungsten–tungsten bond is formally oxidized to yield the corresponding alkylidyne complexes.[6a,6c,6h] Nevertheless, the range of convenient alcohols is limited because they require a minimum steric bulk to prevent deactivation by bridging ligands, and need to comply with the electronic characteristics for catalytic activity. Moreover, because of overcrowding, not every bulky ligand is able to substitute completely all the dimethylamido ligands.

A less investigated tungsten alkylidyne precursor is $[RC{\equiv}W(NMe_2)_3]$ (**4a**, R = *t*Bu; **4b**, R = Et), which combines the advantage of ligand substitution via alcoholysis with the presence of an alkylidyne moiety so that the steric hindrance associated with ditungsten species is reduced. This type of complex was first synthesized by Schrock by salt metathesis of $(NEt_4)[Me_3CC{\equiv}W(Cl)_4]$ (**5**)[10] or $[EtC{\equiv}W(O\text{-}tBu)_3]$ (**6a**) with $LiNMe_2$ (Scheme 2, top).[6a,11] An alternative was reported by McElwee-White, who synthesized $[N{\equiv}W(NMe_2)_3]$ (**4c**) from $[N{\equiv}W(O\text{-}tBu)_3]$ (**7**) in a ligand exchange reaction with 0.75 equivalents of $[Zr(NMe_2)_4]$ or $[Ti(NMe_2)_4]$ (Scheme 2).[12] However, the attention in those years was focused on the "high-oxidation-state" route, and so compounds **4a** and **4b** were neglected, although alcoholysis is an established method to exchange arylamido ligands in analogous molybdenum alkylidyne complexes.[13] Compound **4c** is used in another context to create tungsten oxide surfaces and nanotubes.[14]

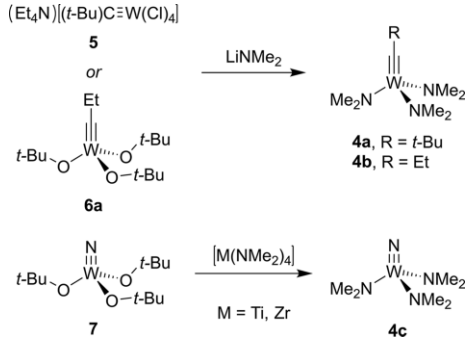

Scheme 2. Synthetic strategies of tris(dimethylamido)tungsten complexes.

This old, yet interesting precursor is perfectly suited to synthesize hybrid, "push-pull" systems; these are metal alkylidyne compounds carrying two electron-withdrawing ligands and one-electron donating ligand, and have proved to be very efficient in alkyne metathesis.[2d,2e,5c,15] Such complexes were constructed in two steps from **1** or **2** via salt metathesis with $M(OC(CF_3)_2Me)$ (M = Li or K) to give $[RC{\equiv}W(dme)\{OC(CF_3)_2Me\}_3]$ (**8a**, R = *t*Bu; **8b**, R = Ar). Subsequent addition of lithium imidazolin-2-iminato salts resulted in the substitution of one alkoxide group and the formation of "push-pull" systems **9a** and **9b** (Scheme 3).

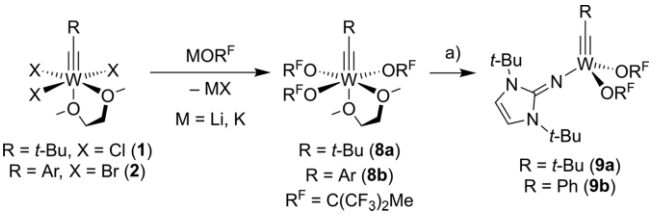

Scheme 3. Classical synthesis of "push-pull" complexes **9**; conditions: a) lithium 1,3-di-*tert*-butylimidazolin-2-iminato, – $LiOR^F$, – DME.

A potentially easier way to generate mixed ligand systems involves the alcoholysis of **4a**[10] or **4b**.[11] Thus, partial substitution of the dimethylamido ligands would result in complexes of the form $[RC{\equiv}W(NMe_2)_n(OR')_{3-n}]$ (n = 1, 2), which combine, respectively, one or two electron-donating ligands (NMe_2) with two or one electron-withdrawing ligands (OR'). We investigated these reactions employing fluorinated *tert*-butoxides ($OC(CF_3)Me_2$, $OC(CF_3)_2Me$, and $OC(CF_3)_3$) and siloxy-based ligands ($OSiPh_3$ and $OSi(O\text{-}tBu)_3$). This ligand selection was guided by the special abilities of tungsten and molybdenum complexes supported by such ligands. For example, $[PhC{\equiv}W\{OSi(O\text{-}tBu)_3\}_3]$ (**10**) is able to perform efficiently alkyne and 1,3-diyne metathesis,[16] whereas $[MesC{\equiv}W\{OC(CF_3)Me_2\}_3]$ (**11**)[17] and $[MesC{\equiv}Mo\{OC(CF_3)_2Me\}_3]$ (**12**)[18] are excellent catalysts for internal and terminal alkyne metatheses. Moreover, related ether[19] and *N*-heterocyclic carbene[20] adducts have been employed in ring-opening alkyne metathesis polymerisation or alkyne homometathesis reactions. Molybdenum complexes of the type $[ArC{\equiv}Mo(OSiPh_3)_3]$ (**13**)[21] proved to be all-rounders and perform comparatively well not only in internal and terminal alkyne metathesis,[22] but also in ring-closing diyne metathesis.[23] Interestingly, their tungsten equivalents[21] are so far unknown.

Results and Discussion

Preparation and Characterization of Complex 4d

Alkylidyne complex $[PhC{\equiv}W(NMe_2)_3]$ (**4d**) was targeted as a precursor for the synthesis of mixed ligand complexes. Its synthesis was optimized from methods reported by Schrock and McElwee-White (see Scheme 2). In a first attempt, Schrock's salt metathesis procedure was adapted. Thus, the *tert*-butoxide ligands in $[PhC{\equiv}W(O\text{-}tBu)_3]$ (**6b**)[6a,6c,24] were substituted at ambient temperature employing three equivalents of $LiNMe_2$ (Scheme 4). On the following day, the solvent was removed at 0 °C to prevent sublimation of volatile **4d**, which was then extracted with cold pentane. The by-product of the reaction,

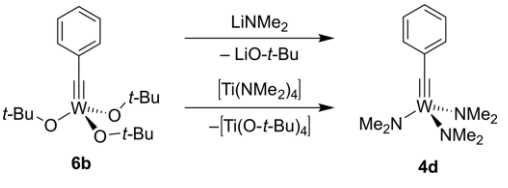

Scheme 4. Synthesis of triamido precursor **4d**.

Full Paper
doi.org/10.1002/ejic.202000835

LiO-*t*Bu, was filtered off, and complex **4d** was isolated from the filtrate in 70 % yield as a yellow powder.

In the second procedure, following McElwee-White, oxophilic tetrakis(dimethylamido)titanium promoted the ligand exchange to generate **4d** in 60 % yield after 2 h under mild conditions (Scheme 4). The ^{1}H NMR spectrum exhibited the characteristic signals for the phenyl group in the aromatic region (6.92–7.36 ppm) and a singlet at 3.38 ppm corresponding to the amido methyl groups. All necessary resonances were also observed in the ^{13}C NMR spectrum. In particular, the methyl groups appeared at 49.8 ppm, and the alkylidyne carbon atom (W≡C) was considerably more deshielded (276.4 ppm) than in **6b** (257 ppm)[24a] but less deshielded than in Schrock's complex **4a** (288.3 ppm).[10] Single crystals suitable for X-ray diffraction analysis were obtained from a solution of **4d** in dichloromethane at –35 °C; the structure is presented in Figure 1.

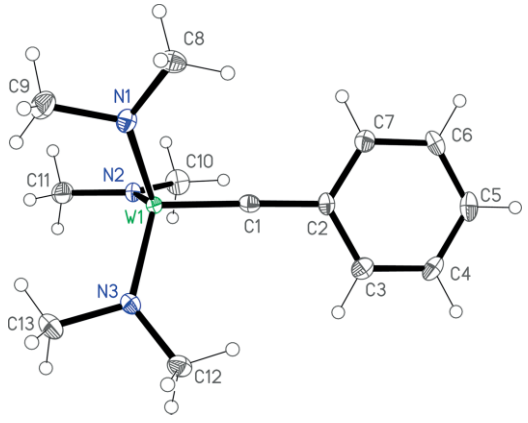

Figure 1. Molecular structure of **4d** with thermal displacement parameters drawn at the 50 % probability level. Relevant bond lengths [Å] and angles [deg]: W1–C1 1.757(3), W1–N1 1.948(3), W1–N2 1.947(3), W1–N3 1.957(3), C1–C2 1.456(4); W1–C1–C2 174.8(2), C1–W1–N1 104.03(12), C1–W1–N2 101.51(12), C1–W1–N3 103.61(12), N1–W1–N2 115.32(11), N1–W1–N3 114.46(11), N2–W1–N3 115.40(11).

Complex **4d** crystallized in the orthorhombic space group *Pbca*. The geometry of the complex is best described as distorted trigonal pyramidal (τ_4 = 0.917(2)),[25] whereby the three nitrogen atoms form the base with N–W–N angles between 114.46(11)° and 115.40(11)°, and the alkylidyne group occupies the apical position (C–W–N angles between 101.51(12)° and 104.03(12)°). The W1–C1 bond length of 1.757(3) Å is virtually equal to that of **6b** (1.758(5) Å).[24b] The nearly linear angle W1–C1–C2 (174.8(2)°) is in accordance with the triple bond character of the alkylidyne moiety. The W–N distances of 1.947(3)–1.957(3) Å are in the expected range for an amide bond.[26] In addition, a second polymorph of **4d** crystallized from a cold pentane solution in the orthorhombic space group *Pnma*. The structure (see Figure S1) displays C_s symmetry, with the asymmetric unit containing only half a molecule. Structural parameters are similar to the first polymorph except for a shorter W1–C1 bond of 1.713(8) Å, and an elongated C1–C2 bond (1.478(10) Å).

Preparation and Characterization of Complexes [PhC≡W(NHMe$_2$)(NMe$_2$)(OR^F)$_2$]

The combination of electron-withdrawing fluorinated ligands and electron-donating amido ligands should provide a basis for the desired "push-pull" effect. Thus, addition of two equivalents of 1,1,1-trifluoro-, 1,1,1,3,3,3-hexafluoro-, or nonafluoro-*tert*-butanol to a solution of **4d** yielded the corresponding disubstituted complexes [PhC≡W(NHMe$_2$)(NMe$_2$)(OR^F)$_2$] in moderate to excellent yields (**14a**, R^F = C(CF$_3$)Me$_2$, 53 %; **14b**, R^F = C(CF$_3$)$_2$Me, 94 %; **14c**, R^F = C(CF$_3$)$_3$, 94 %; Scheme 5, center). It should be noted that one dimethylamine molecule – released as a by-product – remained coordinated, giving pentacoordinate tungsten complexes.

^{1}H NMR spectroscopy of compounds **14a**, **14b** (in C$_6$D$_6$), and **14c** (in [D$_8$]toluene) showed two singlets for the methyl groups of the amido ligands (at 2.75, 2.87 and 3.05 ppm, and at 3.99, 4.05 and 4.34 ppm, respectively), which suggests a hindered rotation around the W–N bonds. A similar situation was observed for the dimethylamine moiety, which gave rise to a broad singlet at 2.19 ppm for **14a**, and to two singlets in the other congeners (**14b**: 2.15 and 2.18 ppm; **14c**: 2.26 and 2.28 ppm). The corresponding amine protons featured chemical shifts of 2.19 ppm (**14a**), 2.47 ppm (**14b**), and 2.75 ppm (**14c**), which, as observed for all other resonances, increased with the degree of fluorination. Furthermore, while the diastereotopic methyl groups of the trifluorinated alkoxide ligands in complex

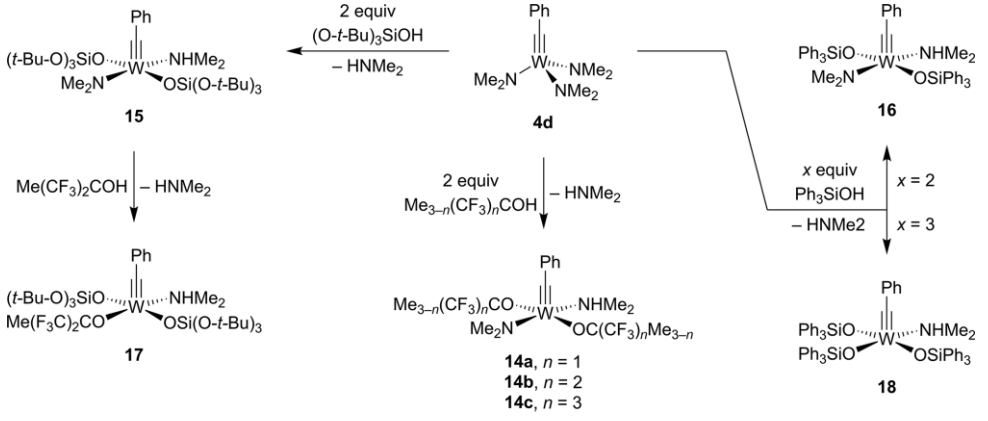

Scheme 5. Synthesis of mixed ligand complexes **14a**–**14c**, **15**–**18**.

Full Paper
doi.org/10.1002/ejic.202000835

14a produced two resonances at 1.26 and 1.54 ppm, the methyl protons of the $OC(CF_3)_2Me$ fragments in complex **14b** appeared as a single multiplet at 1.49 ppm. These observations indicate a C_s molecular symmetry with a *trans* coordination of the alkoxide ligands. Accordingly, only one singlet was observed in the $^{19}F\{^1H\}$ NMR spectra of **14a** (–82.30 ppm) and **14c** (–73.3 ppm), whereas two quartets at –78.4 and –77.2 ppm ($^4J_{FF}$ = 9.7 Hz) were assigned to the diastereotopic CF_3 groups in complex **14b**.

In the $^{13}C\{^1H\}$ NMR spectra of **14a**, **14b**, and **14c**, the alkylidyne carbon atoms resonate at low field at 271.1, 273.4, and 279.1 ppm, respectively. Because of the hindered rotation around the W–N bonds, the methyl groups of the amido ligands appeared as two singlets at 43.4 and 59.4 ppm (**14a**), 42.1 and 59.4 ppm (**14b**), and 41.7 and 59.6 ppm (**14c**). In contrast, the amine moieties gave rise to only one broadened resonance at 40.0, 39.9, and 40.0 ppm, respectively. The crystal structure determination of compound **14b** was attempted, and it verified the *trans* configuration of the fluorinated ligands (see Supporting Information, Figure S2). Unfortunately, the results were unsatisfactory; in particular, the hydrogen atom of the proposed dimethylamine ligand was not located.

In order to get a satisfactory crystal structure, replacement of the amine ligand in **14b** was attempted (see the Supporting Information for details, pp S3–S4). By reaction with DME a few crystals were obtained; however, X-ray crystallographic analysis revealed a dimeric structure (complexes *cis*-**S1** and *trans*-**S1**; see Figures S3–S4), in which the amine ligand is still coordinated, and two methoxy groups bridge the tungsten complexes. These methoxy fragments may have originated from activation of a DME molecule, which substituted one alkoxide ligand and the amido ligand.

Preparation and Characterization of Complexes [PhC≡W(NHMe$_2$)(NMe$_2$)(OSiR$_3$)$_2$]

Siloxy-based catalysts, as demonstrated by 1,3-dyine metathesis promoter **10**[15f,15h,16b] and by Fürstner's complex **13**,[21,27] are highly active and exhibit a remarkable functional group tolerance. Therefore, the combination of these promising silanolate ligands with the amido ligands was also explored. Complexes [PhC≡W(NHMe$_2$)(NMe$_2$)(OSiR$_3$)$_2$] (**15**, R = O-*t*Bu; **16**, R = C_6H_5; Scheme 5, top) were then obtained by slow addition of two equivalents of the corresponding, commercially available alcohols (R_3SiOH) to a solution of **4d** in pentane (**15**) or toluene (**16**). After extraction with pentane, complex **16** was isolated in 91 % yield as a deep green powder, whereas complex **15** was recrystallized from diethyl ether at –35 °C to give orange crystals in 85 % yield.

The ^1H NMR spectra of both compounds show the characteristic splitting of the methyl groups of the amino and the amido moieties, and a general shift into the high field in complex **16** (NH*Me*$_2$: 2.73, 2.75 (**15**), 2.13, 2.15 (**16**) ppm; N*Me*$_2$: 3.29, 4.41 (**15**), 2.75, 3.90 (**16**) ppm; N*H*Me$_2$: 4.86 (**15**), 2.29 (**16**) ppm). In comparison with complexes **14a**–**14c** all resonances in **15** are clearly more deshielded, which can be ascribed to the higher electronegativity of the OSi(O-*t*Bu)$_3$ ligands and, hence, a higher electron-pushing effect of the amido ligand. In contrast, the electronic situation in **16** is very similar to that of complex **14a**, and the carbon resonances seem scarcely affected by the supporting ligands. The silanolate ligands in both complexes give only one set of signals in the ^{13}C NMR spectrum, which indicates the chemical equivalency of these ligands and is consistent with C_s symmetric structures in solution.

Crystallographic analysis of complexes **15** and **16** was frustrated because of poor crystal quality and, again, the indistinguishable amido–amino situation, but the expected *trans* arrangement of the silanolate ligands could be established. The molecular configuration of complex **15** was confirmed chemically by treatment of **15** with $Me(CF_3)_2COH$, which selectively substituted the basic amido ligand (Scheme 5, left). Complex [PhC≡W(NHMe$_2$){OC(CF$_3$)$_2$Me}{OSi(O-*t*Bu)$_3$}$_2$] (**17**) precipitated as orange crystals from a pentane solution at –35 °C in 75 % yield. The crystals are triclinic (space group $P\bar{1}$) and contain two independent molecules per unit cell. The molecular structure (Figure 2) shows a distorted square pyramidal geometry around the tungsten atom (τ_5 = 0.333(5) and 0.324(4))[28] with the alkylidyne moiety in the apical position and proves that the amine ligand is still coordinated. The siloxy ligands are aligned *trans* to each other, but at an angle that deviates strongly from 180° (142.98(14) Å, 143.38(12) Å). The W1–C1 bond length of 1.762(5) Å and 1.752(4) Å is typical for a tungsten alkylidyne bond. The angles between C1 and the alkoxide ligands are particularly wide (104.26°–107.60°), and the W–O distances are significantly elongated (1.918(3)–1.942(3)), probably because of steric hindrance.

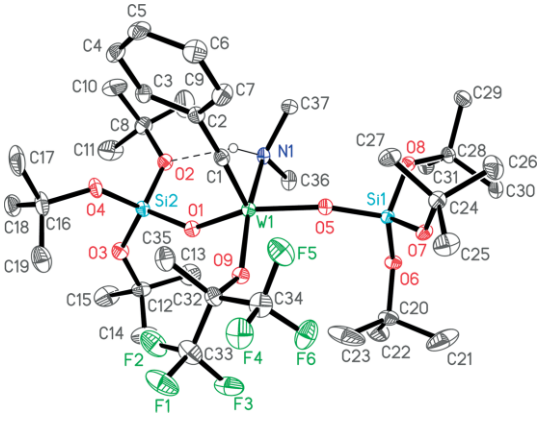

Figure 2. Molecular structure of one of the two independent molecules of **17** with thermal displacement parameters drawn at the 30 % probability level; hydrogen atoms (except at N1) are omitted for clarity. Relevant bond lengths [Å] and angles [deg]: W1–C1 1.762(5), W1′–C1′ 1.752(4), W1–N1 2.234(4), W1′–N1′ 2.231(4), W1–O1 1.937(3), W1′–O1′ 1.942(3), W1–O5 1.918(3), W1′–O5′ 1.918(3), W1–O9 1.939(3), W1′–O9′ 1.933(3), C1–C2 1.438(7), C1′–C2′ 1.457(6); W1–C1–C2 177.6(4), W1′–C1′–C2′ 175.7(4), C1–W1–N1 92.66(18), C1′–W1′–N1′ 92.78(17), C1–W1–O1 106.63(17), C1′–W1′–O1′ 105.18(16), C1–W1–O5 106.60(16), C1′–W1′–O5′ 107.60(16), C1–W1–O9 104.26(17), C1′–W1′–O9′ 104.26(17), N1–W1–O1 80.83(13), N1′–W1′–O1′ 80.69(13), N1–W1–O5 81.80(13), N1′–W1′–O5′ 81.83(13), N1–W1–O9 162.97(15), N1′–W1′–O9′ 162.81(13), O1–W1–O5 142.98(14), O1′–W1′–O5′ 143.38(12), O1–W1–O9 92.30(12), O1′–W1′–O9′ 92.49(12), O5–W1–O9 94.94(12), O5′–W1′–O9′ 94.89(12). Values for the second molecule are distinguished by primes.

Substitution of the amido group by the fluorinated alkoxide (δ_H = 2.03 ppm, δ_F = –76.2 ppm) is also observed by NMR spectroscopy. In addition, the amine protons are considerably

Full Paper
doi.org/10.1002/ejic.202000835

deshielded. The W≡C signal at 281.3 ppm is slightly low-field shifted compared to **15** (δ_C = 278.1 ppm).

Preparation and Characterization of Complex [PhC≡W(NHMe$_2$)(OSiPh$_3$)$_3$]

So far, tungsten complexes of type [RC≡W(OSiPh$_3$)$_3$] have not been described in the literature. For example, addition of KOSiPh$_3$ to tribromido precursor **2** led to the formation of K[PhC≡W(OSiPh$_3$)$_4$]•dme (dme = 1,2-dimethoxyethane),[21,29] a tungstate complex bearing four siloxy ligands. Instead, reaction of our triamido precursor **4d** with three equivalents of Ph$_3$SiOH in toluene (Scheme 5, bottom right) resulted in the formation of neutral [PhC≡W(NHMe$_2$)(OSiPh$_3$)$_3$] (**18**) in 88 % yield as a brownish-pink solid. As in former complexes **14**–**17**, the NMR spectra indicate one dimethylamine molecule bonded to the metal atom (NH*Me*$_2$, δ_H = 1.80 and 1.82 ppm; N*H*Me$_2$, δ_H = 2.73 ppm). The expected low-field shifted signal for the alkylidyne carbon atom is observed at δ_C = 277.9 ppm. Unfortunately, NMR analyses show that the complex is unstable in solution and slowly decomposes generating hexaphenyldisiloxane (see Figure S17).

Pale red crystals suitable for X-ray diffraction analysis were obtained from a concentrated dichloromethane solution at –35 °C; the structure is displayed in Figure 3. The compound crystallizes in the monoclinic space group *C*2/*c*, and its coordination geometry can be described as distorted square-pyramidal (τ_5 = 0.263(4), base angles 144.59(11)° and 160.37(12)°).[28] The alkylidyne moiety occupies the apical position with a normal W–C triple bond length of 1.762(4). The W–N bond (2.250(3) Å) is moderately elongated compared to complex **17** (2.23 Å), which is probably associated with the increased size of the third alkoxide ligand.

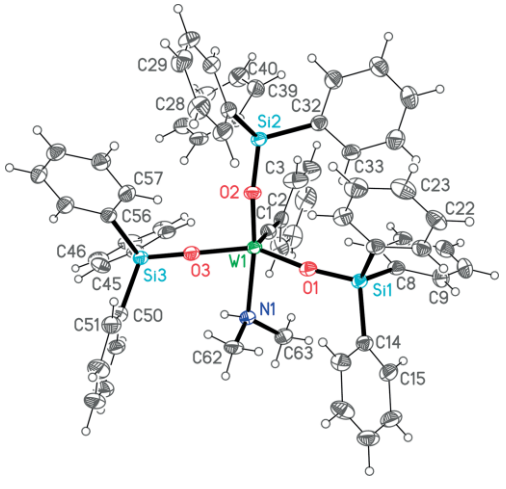

Figure 3. Molecular structure of **18**•(CH$_2$Cl$_2$)$_{3.5}$ with thermal displacement parameters drawn at the 50 % probability level; co-crystallized dichloromethane molecules are omitted for clarity. Relevant bond lengths [Å] and angles [deg]: W1–C1 1.762(4), W1–N1 2.250(3), W1–O1 1.927(3), W1–O2 1.939(3), W1–O3 1.941(3), C1–C2 1.458(6); W1–C1–C2 177.6(4), C1–W1–N1 94.05(16), C1–W1–O1 106.17(16), C1–W1–O2 105.48(15), C1–W1–O3 104.79(16), N1–W1–O1 81.95(12), N1–W1–O2 160.37(12), N1–W1–O3 79.13(12), O1–W1–O2 94.18(12), O1–W1–O3 144.59(11), O2–W1–O3 93.75(12).

Preparation of Tetrakis(dimethylamido)bis(fluoro-*tert*-butoxide)ditungsten Complexes

Attempts to prepare inverse push-pull analogs – containing two amido ligands and one alkoxide substituent – of complexes **14**–**16** from **4d** were unsuccessful, and resulted only in the known disubstitution reactions, but with halved yields. A valid alternative was found in the ditungsten route. Through direct alcoholysis of bimetallic complex **3a**, compounds of the type [W$_2$(NMe$_2$)$_2$(OR^F)$_4$] were successfully prepared using four equivalents or an excess of the alcohol (R^{F}OH).[6f,9,30] In line with this, we expected substitution of just two amido ligands to be possible if only two equivalents of the fluorinated alcohols were used (Scheme 6). Indeed, after sublimation of the crude products at 120 °C, compounds with the formula [W$_2$(NMe$_2$)$_4$(OR^F)$_2$] were isolated as yellow to orange solids in good yields (**19a**, R^F = C(CF$_3$)Me$_2$, 68 %; **19b**, R^F = C(CF$_3$)$_2$Me, 60 %; **19c**, R^F = C(CF$_3$)$_3$, 70 %).

The NMR spectra (Supporting Information, pp S30–S33) show a series of diastereoisomers, which prevents signal assignment, but integration of the characteristic regions in the ^{1}H NMR spectra is consistent with the substitution of two amido ligands in **3a** and the expected formation of complexes **19a**–**19c**. Additional evidence for the correct composition was provided by combustion analysis. However, unsymmetrical substitution at the ditungsten core, i.e., 1,1-[W$_2$(NMe$_2$)$_4$(OR^F)$_2$] (*C*$_s$ symmetry), should be also considered. Only in the case of complex **19b**, two singlets at 1.75 and 1.78 ppm for the methyl protons of the alkoxide ligand indicate the existence of mainly two conformers in a 2:1 ratio. In the fluorine NMR spectrum, the major isomer displays a single peak at –78.6 ppm, whereas the CF$_3$ groups of the second isomer split into two quartets at –78.2 and –78.9 ppm and, therefore, they should be diastereotopic. Thus, the latter isomer must be the *C*$_2$-symmetric *rac*-1,2–**19b** (gauche conformation), and the major isomer is probably *meso*-1,2–**19b** (*C*$_{2h}$ symmetry, anti-conformation).

In addition, crystals suitable for X-ray diffraction analysis were grown from a saturated Et$_2$O solution at –35 °C, confirming the structure of complexes **19a**–**19c** (Figure 4, Figure 5, and

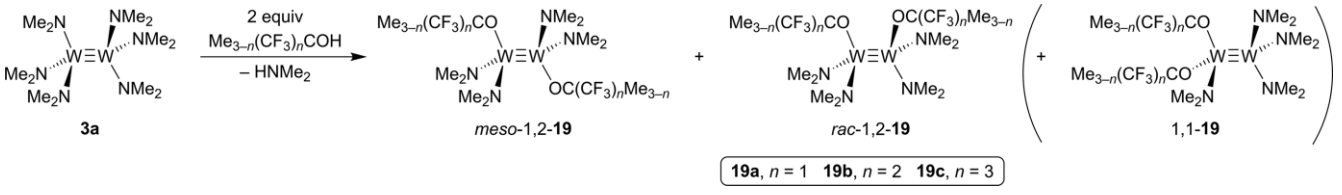

Scheme 6. Synthesis of ditungsten complexes **19a**–**19c** produced a mixture of isomers.

Full Paper
doi.org/10.1002/ejic.202000835

Figure 6). The products crystallized, respectively, in the space groups $P\bar{1}$, $P2_1/n$, and $P2_1/n$, the latter two being isotypic, and they all contain half a molecule in the asymmetric unit (the other half being generated by inversion). All three molecules show a staggered conformation with an anti-periplanar orientation (180°) of the fluorinated ligands. The W1–O1 distances are, respectively, 1.907(2) Å, 1.936(2) Å, and 2.0058(17) Å, with the latter being considerably longer than other reported tungsten–alkoxide bonds (1.868–1.934 Å).[6f,26] The W1–W1# bond lengths (2.3155(3) Å, 2.3144(3) Å, 2.28593(18) Å) are comparable with those of analogous structures[6f,9] and are in the typical range for a tungsten–tungsten triple bond.[31]

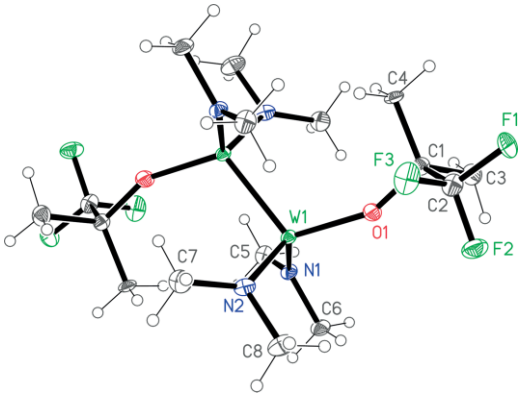

Figure 4. Molecular structure of *meso*-1,2–**19a** with thermal displacement parameters drawn at the 50 % probability level; symmetry operator –*x* + 1, –*y* + 1, –*z* + 2. Only one position of the disordered alkoxide group is shown. Relevant bond lengths [Å] and angles [deg]: W1–W1# 2.3155(3), W1–N1 1.950(3), W1–N2 1.951(3), W1–O1 1.907(2); N1–W1–N2 116.40(12), N1–W1–O1 111.18(12), N1–W1–W1# 102.57(9), N2–W1–O1 111.61(12), N2–W1–W1# 102.06(9), O1–W1–W1# 112.30(8).

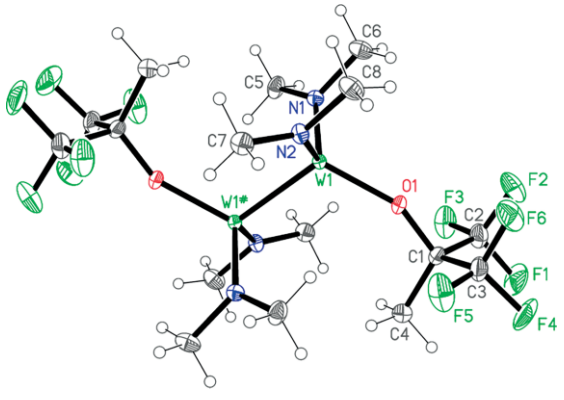

Figure 5. Molecular structure of *meso*-1,2–**19b** with thermal displacement parameters drawn at the 50 % probability level; symmetry operator –*x* + 1, –*y* + 1, –*z* + 1. Relevant bond lengths [Å] and angles [deg]: W1–W1# 2.3144(3), W1–N1 1.940(3), W1–N2 1.932(3), W1–O1 1.936(2); N1–W1–N2 115.51(12), N1–W1–O1 110.34(11), N1–W1–W1# 102.93(9), N2–W1–O1 111.27(11), N2–W1–W1# 102.13(9), O1–W1–W1# 114.27(7).

Despite the molecular structure determinations, the NMR analyses discussed above indicate that the bulk materials consist of isomeric mixtures. Indeed, the gauche conformer of **19a**, *rac*-1,2-$[W_2(NMe_2)_4(OC(CF_3)Me_2)_2]$, was also characterized crystallographically (see Supporting Information, Figure S5). Hence, the structure of compounds **19a**–**19c** is not well-defined. Even

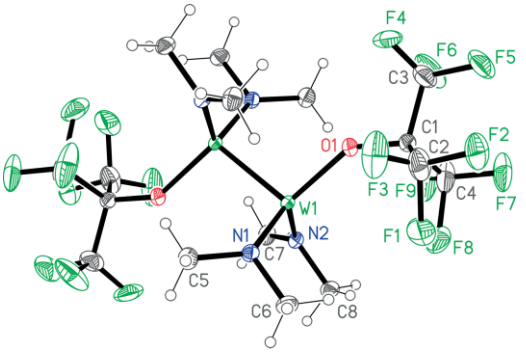

Figure 6. Molecular structure of *meso*-1,2–**19c** with thermal displacement parameters drawn at the 50 % probability level; symmetry operator –*x* + 1, –*y* + 1, –*z* + 1. Only one position of the disordered CF_3 groups is shown. Relevant bond lengths [Å] and angles [deg]: W1–W1# 2.28593(18), W1–N1 1.931(2), W1–N2 1.931(2), W1–O1 2.0058(17); N1–W1–N2 111.84(9), N1–W1–O1 117.61(8), N1–W1–W1# 100.53(6), N2–W1–O1 119.74(8), N2–W1–W1# 100.58(6), O1–W1–W1# 102.01(5).

so, the simple synthetic approach makes these complexes interesting targets as alkyne metathesis promoters, and their catalytic behavior is presented in the next section.

Catalytic Activity in Internal Alkyne Metathesis

The activity of all ten complexes **14**–**19** in alkyne metathesis was investigated with respect to the homodimerization of our benchmark substrate $BnO(CH_2)_2C{\equiv}CMe$ (Bn = benzyl, $C_6H_5CH_2$)[5c] in the presence of molecular sieves under standard conditions (Scheme 7).[15h]

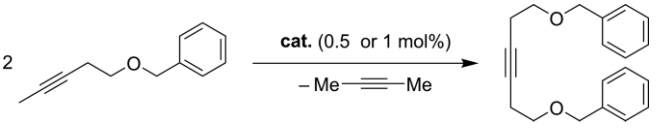

Scheme 7. Self-metathesis of 5-benzyloxy-2-pentyne (250 µmol) catalyzed by complexes **14**–**19** (cat.); conditions: ambient temperature, toluene (1.25 mL), molecular sieves 5 Å (250 mg), *n*-decane (0.05 mL) as internal standard.

For all complexes, the conversion was monitored by GC analyses at specified time intervals, and the results are plotted in Figure 7, Figure 8, and Figure 9. In addition, to confirm the

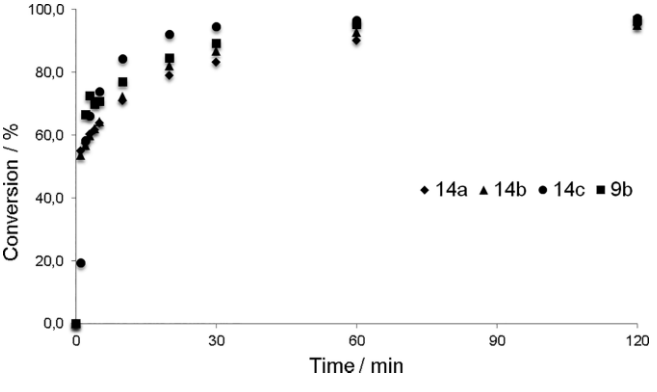

Figure 7. GC conversion–time diagram of the self-metathesis of 5-benzyloxy-2-pentyne using 1 mol-% of **14a**–**14c** (and **9b** for comparison); conditions: see Scheme 7.

Full Paper
doi.org/10.1002/ejic.202000835

maximal conversion, isolated yields were determined for almost all reactions except for the two least active compounds (**17** and **18**); the values are summarized in Table 1 and agree with the GC data.

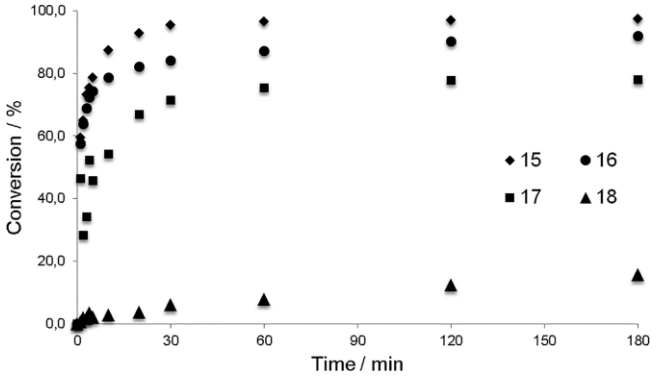

Figure 8. GC conversion–time diagram of the self-metathesis of 5-benzyloxy-2-pentyne using 1 mol-% of **15**–**18**; conditions: see Scheme 7.

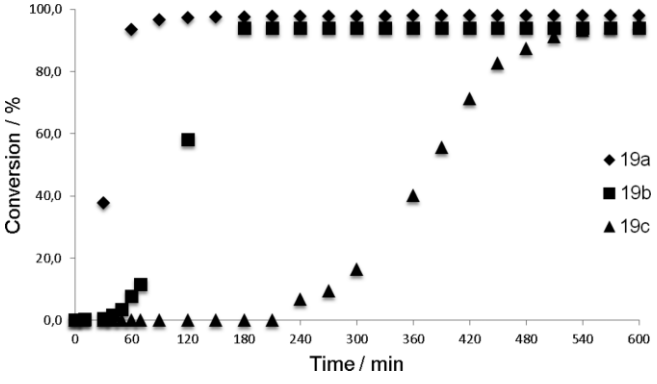

Figure 9. GC conversion–time diagram of the self-metathesis of 5-benzyloxy-2-pentyne using 0.5 mol-% of **19a**–**19c**; conditions: see Scheme 7.

Table 1. GC conversions (%), isolated yields (%), and $TOF_{10\ min}$ (min^{-1}) of the self-metathesis of 5-benzyloxy-2-pentyne using complexes **14**–**19**.

Catalyst	GC conversion [*t*/h][a]	Isolated yield[b]	$TOF_{10\ min}$
14a	95 [2]	93	7.1
14b	93 [2]	94	7.2
14c	97 [2]	96	8.4
15	98 [3]	96	8.7
16	92 [3]	80	7.9
17	78 [3]	n.d.[c]	5.2
18	16 [3]	n.d.[c]	0.2
19a	97 [3]	95	n.d.[c]
19b	92 [4]	91	n.d.[c]
19c	95 [10]	94	n.d.[c]

[a] Calculated from the area counts ratio of the substrate to *n*-decane at time *t*; conditions: ambient temperature, 1 mol-% **14**–**18** or 0.5 mol-% **19a**–**19c**, toluene (1.25 mL), molecular sieves 5 Å (250 mg), *n*-decane (0.05 mL) as internal standard. [b] Conditions as in [a] without *n*-decane, isolated by filtration through Celite and neutral alox followed by column chromatography purification, if necessary. [c] Not determined.

Fluorinated complexes **14a**–**14c** exhibited an almost equivalent reaction progress (Figure 7), and after 2 h reached excellent conversions of 95 %, 93 %, and 97 %, respectively. In contrast to the trend observed for other fluorinated tungsten alkylidyne complexes,[17,18c] the degree of fluorination does not seem to affect the catalytic performance of these systems. Among them, complex **14c** showed the highest activity ($TOF_{10\ min}$ = 8.4 min^{-1}) and its conversion rate is comparable to other push-pull species such as **9b** (see Scheme 3).[5c,32] The gel permeation chromatography (GPC) traces of the crude reaction mixtures (see Figures S22–S26) confirmed full conversion to the dimeric species and the absence of oligomers.

Silanolate-based benzylidyne complexes **15**–**18** behaved substantially differently in the self-metathesis of 5-benzyloxy-2-pentyne (Figure 8). The fastest initiation ($TOF_{10\ min}$ = 8.7 min^{-1}) and highest conversion (97 % in 2 h) was achieved by tri(*tert*-butoxy)silanolate complex **15**. The analogous push–pull complex **16** initiated similarly fast ($TOF_{10\ min}$ = 7.9 min^{-1}) but reached only a lower conversion of about 90 % after 2 h. Substitution of the third amido ligand as in complexes **17** and **18** caused a reduced catalytic performance, probably for steric reasons. A significant activity decrease was observed for triphenylsilanolate-supported complex **18**, which reached only 16 % conversion after 3 h and a 50 % maximum conversion after several days. The reason might be slow deactivation of **18** by the aforementioned formation of hexaphenyldisiloxane. In addition, the GPC trace of the crude reaction mixture after catalysis using complex **18** revealed the production of polymers (see Figure S30).

Bimetallic species **19a**–**19c** are precatalysts that first have to be oxidized by the alkyne to form the corresponding active tungsten alkylidyne complex. This activation step is the rate-determining step and it is relatively slow, so the amount of active species is small at the beginning. As concluded in previous studies,[17,18c,20c] the initiation time increases with the degree of fluorination of the alkoxy ligands (Figure 9), which is consistent with the increasing electrophilicity at the metal cores. Thus, using complex **19a** the alkyne substrate was converted to 93 % within 1 h (according to GC), whereas complex **19b** reached a similar conversion only after about 3 h. Complex **19c** exhibited the longest initiation period (no conversion was detected in the first 4 h), and required 10 h to achieve a conversion of 95 %.

In principle, the series of compounds **19** may be used as two-component systems by in situ generation[13c–13g] from **3a** and the corresponding alcohol. Because of its simplicity, this approach is certainly promising and will be investigated.

Conclusion

Alkyne metathesis promoters featuring a hybrid ligand environment have been readily and selectively synthesized by alcoholysis of tris(dimethylamido) tungsten complexes with silanols and fluorinated *tert*-butanols. Among the tungsten benzylidyne versions (**14**–**18**), the perfluorinated *tert*-butoxide (**14c**) and the tri(*tert*-butoxy)siloxide (**15**) based complexes allowed for nearly full conversion in the self-metathesis of 5-benzyloxy-2-pentyne after 2 h at catalyst loadings of 1 mol-%. In addition, push-pull ditungsten complexes **19a**–**19c** were obtained directly from hexakis(dimethylamido)ditungsten (**3a**), but only 1,1,1-trifluoro-*tert*-butoxide complex **19a** performed efficiently in alkyne me-

tathesis. In future studies, addition of alkynes to open these species and generate alkylidyne complexes will be further investigated. We are optimistic that the present work will increase the popularity of the alcoholysis synthetic approach and the use of amido-supported tungsten precursors in the alkyne metathesis community.

Experimental Section

General. All operations with air- and moisture-sensitive compounds were performed in a glovebox in a dry argon atmosphere (MBraun 200B) or on a high vacuum line using Schlenk techniques. Solvents (except THF) were purified by a solvent purification system (MBraun) and stored over molecular sieves (4 Å) prior to use. THF and deuterated solvents were dried by conventional methods[33] and stored over molecular sieves. Unless otherwise indicated, all starting materials obtained from Sigma-Aldrich, Acros or Chempur were used without further purification. Celite diatomaceous earth was stored for at least 3 d in an oven at 120 °C. Powdered molecular sieves 5 Å (particle size < 50 μm, Sigma-Aldrich) used for alkyne metathesis reactions were dried for at least 24 h at 180 °C under high vacuum prior to use. WCl_4,[8a] $[W_2(NMe_2)_6]$,[7b,7c] $[W_2(O\text{-}t\text{Bu})_6]$,[7c] $[PhC{\equiv}W(O\text{-}t\text{Bu})_3]$,[6a,6c] and $[Ti(NMe_2)_4]$[34] were prepared according to slightly modified literature procedures (see Supporting Information for details, pp S2–S3), and 5-benzyloxy-2-pentyne[5c] was prepared according to the literature procedure.

NMR spectroscopy. NMR spectra were recorded with Bruker DPX 200 (200 MHz, room temperature), Bruker AV II 300 (300 MHz, room temperature), AV III HD 300 (300 MHz, room temperature), and Bruker AV II 600 (600 MHz, 303 K) devices. ^1H and $^{13}C\{^1H\}$ NMR spectra were referenced relative to the (residual) solvent signals. $^{19}F\{^1H\}$ NMR spectra were referenced relative to virtual internal $CFCl_3$ (the observation frequencies of a dilute solution of $CFCl_3$ in the deuterated solvents were determined earlier). Chemical shifts (δ) are expressed in parts per million (ppm). The number of protons (*n*) for a given resonance is indicated by *n*H. The number of protons attached to each carbon atom was determined by ^{13}C-DEPT135 experiments. Coupling constants (*J*) are reported in Hertz (Hz), and splitting patterns are indicated as s (singlet), d (doublet), t (triplet), q (quartet), sep (septet), m (multiplet), and br (broad).

X-ray Diffraction Studies

Single crystals were examined and mounted in perfluorinated inert oil and transferred to the cold gas stream of the diffractometer. Data were recorded on an Oxford Diffraction Nova A diffractometer, using mirror-focused Cu-K_α radiation (1.54184 Å; compound **18**) or an Oxford Diffraction Xcalibur Eos diffractometer using graphite-monochromated Mo-K_α radiation (0.71073 Å; compounds **4d** (both polymorphs), **14b**, **17**, *meso*-1,2–**19a**, *rac*-1,2–**19a**, **19b**, **19c**, *cis*-**S1**, *trans*-**S1**). Absorption corrections were performed on the basis of multiscans. All structures were solved using SHELXS-97[35] and refined anisotropically by full-matrix least-squares procedures on F^2 using the SHELXL-2018/3 program.[36] Hydrogen atoms were either located and refined isotropically (amine proton in compounds **17**, **18**, *cis*-**S1**, and *trans*-**S1**), included as idealized methyl groups allowed to rotate but not tip (all methyls with the exception of disordered methyl groups in *meso*-1,2–**19a** and in compound *cis*-**S1**), or placed geometrically and allowed to ride on their attached carbon atoms (all other H atoms). If possible, disordered groups were refined on two or more positions; appropriate restraints were employed to improve refinement stability, but the dimensions of disordered groups should always be interpreted with caution. Crystallographic parameters and further structural details are summarized in the Supporting Information (Table S1, pp S5–S7; for special features and exceptions, see pp S7–S8). The program *XP* (Siemens)[37] was used for graphical representations.

Deposition Numbers 2026935 (for **4d**, *Pbca* polymorph), 2026936 (for **4d**, *Pnma* polymorph), 2026937 (for **14b**), 2026938 (for *cis*-**S1**), 2026939 (for *trans*-**S1**), 2026940 (for **17**), 2026941 (for **18**), 2026942 (for *meso*-1,2–**19a**), 2026943 (for *rac*-1,2–**19a**), 2026944 (for **19b**), 2026945 (for **19c**) contain the supplementary crystallographic data for this paper. These data are provided free of charge by the joint Cambridge Crystallographic Data Centre and Fachinformationszentrum Karlsruhe Access Structures service www.ccdc.cam.ac.uk/structures.

Other analytical techniques. Elemental analyses (C, H, N) were determined by combustion and gas chromatographic analysis on a Vario MICRO cube (Elementar) instrument equipped with WLD and IR detectors using argon as carrier gas. Values are reported in % and as an average of three runs. Gas chromatography (GC) analyses were executed on a Shimadzu GC2010 device equipped with a Zebron ZB-5MS column (30 m × 0.25 mm × 0.25 μm) and FID detector. Samples (1 μL) were injected at 250 °C with a split/splitless ratio of 1:10 and heated in the column from 50 to 300 °C with a heating rate of 10 °C min^{-1} and using helium as carrier gas (30 cm s^{-1}). For calibration, *n*-decane was used as an internal standard. GPC analyses were performed at 35 °C at a flow rate of 1 mL/min through PSS SDV (Lux) THF-GPC columns (5 μm, 100 Å and 1000 Å) using a light scattering detector (Agilent Series 1200) and a polystyrene standard for calibration.

Experimental details

$[PhC{\equiv}W(NMe_2)_3]$, 4d. The preparation was based on published syntheses by Schrock[11] or McElwee-White.[12] *Based on McElwee-White's route:* $[Ti(NMe_2)_4]$ (0.75 equiv., 341.6 mg, 1.5238 mmol) was added to a solution of $[PhC{\equiv}W(O\text{-}t\text{-}Bu)_3]$ (1000 mg, 2.031 mmol) in Et_2O (60 mL). After stirring for 2 h at ambient temperature the solution was cooled to 0 °C in an ice-water bath. The solvent was then removed carefully under reduced pressure to prevent sublimation of $[PhC{\equiv}W(NMe_2)_3]$. The resulting gray-brown residue was suspended in small amounts of cold *n*-pentane, stirred for 5 min, and collected on a frit. The collected solid was washed three times with small amounts of cold *n*-pentane and dried under vacuum to obtain a deep yellow powder in 60 % yield (493.8 mg, 1.2187 mmol). *Based on Schrock's route:* $LiNMe_2$ (3.05 equiv., 316 mg, 6.19 mmol) was added in portions to a stirred solution of $[PhC{\equiv}W(O\text{-}t\text{-}Bu)_3]$ (1000 mg, 2.031 mmol) in Et_2O (60 mL). The reaction mixture was stirred overnight at ambient temperature and then cooled to 0 °C in an ice-water bath. The solvent was removed under reduced pressure, and the residue was suspended in small amounts of cold *n*-pentane, stirred for 5 min, and collected on a frit. The collected solid was washed three times with small amounts of cold *n*-pentane and dried under vacuum. The product was isolated as a deep yellow powder in 70 % yield (576 mg, 1.422 mmol). Crystals suitable for X-ray diffraction analysis were obtained from a concentrated solution in dichloromethane (P_{bca} polymorph) or *n*-pentane (*Pnma* polymorph) at −35 °C. **^1H NMR** (300.1 MHz, C_6D_6): δ = 3.38 (s, 18H; $6 \times CH_3$), 6.92 (tt, $^3J_{H,H}$ = 7.4 Hz, $^4J_{H,H}$ = 1.3 Hz, 1H; *para*-*H*), 7.17–7.24 (m, 2H; Ar-*H*), 7.30–7.36 (m, 2H, Ar-*H*); **^{13}C NMR** (75.5 MHz, C_6D_6): δ = 49.8 (CH_3), 125.5 (Ar-CH), 127.9 (Ar-CH), 130.4 (Ar-CH) 148.2 (Ar-C_q), 276.4 (W≡C); **elemental analysis** calcd. (%) for $C_{13}H_{23}N_3W$: C 38.54, H 5.72, N 10.37; found C 38.18, H 5.65, N 10.13.

$[PhC{\equiv}W(NHMe_2)(NMe_2)\{OC(CF_3)Me_2\}_2]$, 14a. A solution of 1,1,1-trifluoro-*tert*-butanol (2.0 equiv., 128.4 mg, 1.002 mmol) in a small

Full Paper
doi.org/10.1002/ejic.202000835

amount of *n*-pentane was added slowly to a solution of **4d** (203.0 mg, 501.0 μmol) in *n*-pentane (15 mL). After stirring the reaction mixture for 3 h at ambient temperature, the solvent was removed under reduced pressure. The residue was dissolved in a small amount of diethyl ether and stored in a freezer at –35 °C, which resulted in precipitation of the product as yellow needles. The mother liquor was removed by decantation, and the crystals were dried in high vacuum. Yield: 53 % (163.9 mg, 265.9 μmol). **^{1}H NMR** (600.1 MHz, C_6D_6): δ = 1.26 (s, 6H; 2 × C(CF_3)Me(CH_3)), 1.54 (s, 6H; 2 × C(CF_3)(CH_3)Me), 2.19 (br s, 7H; N*H*(CH_3)$_2$), 2.75 (s, 3H; NMe(CH_3)), 3.99 (s, 3H; N(CH_3)Me), 6.82 (tt, $^3J_{H,H}$ = 7.4 Hz, $^4J_{H,H}$ = 1.3 Hz, 1H; *para-H*), 6.98–7.01 (m, 2H; Ar-*H*), 7.17–7.21 (m, 2H; Ar-*H*); **^{13}C NMR** (150.9 MHz, C_6D_6): δ = 25.6 (C(CF_3)(CH_3)Me), 25.9 (C(CF_3)Me(CH_3)), 40.0 (br, $NHMe_2$), 43.4 (NMe(CH_3)), 59.4 (N(CH_3)Me), 79.3 (q, $^2J_{C,F}$ = 27.6 Hz; *C*(CF_3)Me$_2$), 126.0 (*para-C*H), 127.8 (*ortho-C*H), 128.9 (q, $^1J_{C,F}$ = 273 Hz; *C*F_3), 131.2 (*meta-C*H), 147.5 (*ipso-C*$_q$), 271.1 (W≡*C*); **^{19}F NMR** (376.8 MHz, C_6D_6): δ = –83.02*;* **elemental analysis** calcd. (%) for $C_{19}H_{30}F_6N_2O_2W$: C 37.03, H 4.91, N 4.55; found C 36.63, H 4.67, N 4.31.

[PhC≡W(NHMe$_2$)(NMe$_2$){OC(CF$_3$)$_2$Me}$_2$], 14b. A solution of 1,1,1,3,3,3-hexafluoro-2-methylpropan-2-ol (2.0 equiv., 269.6 mg, 1.481 mmol) in a small amount of *n*-pentane was added slowly to a solution of **4d** (300 mg, 740.4 μmol) in *n*-pentane (20 mL). After stirring the reaction mixture for 3 h at ambient temperature, the solvent and unreacted starting materials were removed under reduced pressure, which resulted in a pale brown solid. Yield: 94 % (504.0 mg, 696.0 μmol). **^{1}H NMR** (300.1 MHz, C_6D_6): δ = 1.49 (m, 6H; 2 × C(CF_3)$_2$CH_3), 2.15 (s, 3H; NH(CH_3)Me), 2.18 (s, 3H; NHMe(CH_3)), 2.47 (br s, 1H; N*H*Me$_2$), 2.87 (s, 3H; N(CH_3)Me), 4.05 (s, 3H; NMe(CH_3)), 6.79 (tt, $^3J_{H,H}$ = 7.4 Hz, $^4J_{H,H}$ = 1.3 Hz, 1H; *para-H*), 6.94–7.02 (m, 2H; Ar-*H)*, 7.11–7.21 (m, 2H; Ar-*H*); **^{13}C NMR** (75.5 MHz, C_6D_6): δ = 20.2 (C(CF_3)$_2$(CH_3)), 39.9 ($NHMe_2$), 42.1 (N(CH_3)Me), 59.4 (NMe(CH_3)), 81.5 (sept, $^2J_{C,F}$ = 28 Hz; *C*(CF_3)$_2$Me), 124.5 (q, $^1J_{C,F}$ = 288 Hz; 2 × *C*F_3), 125.3 (q, $^1J_{C,F}$ = 289 Hz; 2 × *C*F_3), 127.1 (Ar-*C*H), 127.9 (Ar-*C*H), 131.5 (Ar-*C*H), 146.4 (Ar-*C*$_q$), 273.4 (W≡*C*). **^{19}F NMR** (188.3 MHz, C_6D_6): δ = –78.4 (q, $^4J_{F,F}$ = 9.7 Hz, 6F; 2 × CF_3) –77.2 (q, $^4J_{F,F}$ = 9.7 Hz, 6F; 2 × CF_3); **elemental analysis** calcd. (%) for $C_{19}H_{24}F_{12}N_2O_2W$: C 31.51, H 3.34, N 3.87; found C 31.29, H 3.20, N 3.92.

[PhC≡W(NHMe$_2$)(NMe$_2$){OC(CF$_3$)$_3$}$_2$], 14c. A solution of perfluoro-*tert*-butanol (2.0 equiv., 156.1 mg, 0.661 mmol) in a small amount of toluene was added slowly to a solution of **4d** (134.0 mg, 330.7 μmol) in toluene (10 mL). After stirring the reaction mixture for 3 h at ambient temperature, the solvent and unreacted starting materials were removed under reduced pressure, which resulted in a pale brown solid. Yield: 94 % (258.9 mg, 311.1 μmol). **^{1}H NMR** (300.3 MHz, [D$_8$]toluene): δ = 2.26 (s, 3H; NH(CH_3)Me), 2.28 (s, 3H; NHMe(CH_3)), 2.75 (br s, 1H; N*H*Me$_2$), 3.05 (s, 3H; N(CH_3)Me), 4.34 (s, 3H; NMe(CH_3)), 6.73 (tt, $^3J_{H,H}$ = 7.4 Hz, $^4J_{H,H}$ = 1.3 Hz, 1H; *para-H*), 6.94–7.03 (m, 2H; Ar-*H)*, 7.06–7.15 (m, 2H; Ar-*H*); **^{13}C NMR** (75.5 MHz, [D$_8$]toluene): δ = 40.0 ($NHMe_2$), 41.7 (N(CH_3)Me), 59.6 (NMe(CH_3)), 83.0 (m; *C*(CF_3)$_3$), 122.0 (q, $^1J_{C,F}$ = 294 Hz; *C*F_3), 127.5 (Ar-*C*H), 132.3 (Ar-*C*H), 145.4 (Ar-*C*$_q$), 279.1 (W≡*C*), the resonance for one aryl-*C*H carbon atom overlaps with the solvent signal and was not observed; **^{19}F NMR** (282.5 MHz, [D$_8$]toluene): δ = –73.3 (CF_3); **elemental analysis** calcd. (%) for $C_{19}H_{18}F_{18}N_2O_2W$: C 27.42, H 2.18, N 3.37; found C 27.46, H 2.19, N 3.32.

[PhC≡W(NHMe$_2$)(NMe$_2$){OSi(O-*t*-Bu)$_3$}$_2$], 15. A solution of (*t*BuO)$_3$SiOH (2.0 equiv., 261.1 mg, 987.2 μmol) in a small amount of *n*-pentane was added slowly to a solution of **4d** (200.0 mg, 493.6 μmol) in *n*-pentane (20 mL). The reaction mixture was stirred for 2 h at ambient temperature, concentrated under reduced pressure, and stored at –35 °C. The product was isolated as orange crystals in 85 % yield (373.0 mg, 419.6 μmol). **^{1}H NMR** (300.1 MHz, C_6D_6): δ = 1.48 (s, 54H; 6 × OC(CH_3)$_3$), 2.73 (s, 3H; NH(CH_3)Me), 2.75 (s, 3H; NHMe(CH_3)), 3.29 (s, 3H; N(CH_3)Me), 4.42 (s, 3H; NMe(CH_3)), 4.86 (br m, 1H; N*H*Me$_2$), 6.77–6.85 (m, 1H; *para-H*), 7.24–7.33 (m, 4H; 4 × Ar-*H*); **^{13}C NMR** (75.5 MHz, C_6D_6): δ = 31.9 (OC(CH_3)$_3$), 40.8 (NH(CH_3)$_2$), 43.6 (N(CH_3)Me), 60.6 (NMe(CH_3)), 72.3 (O*C*Me$_3$), 125.5 (Ar-*C*H), 127.1 (Ar-*C*H), 132.5 (Ar-*C*H), 147.7 (Ar-*C*$_q$), 278.1 (W≡*C*); **elemental analysis** calcd. (%) for $C_{35}H_{72}N_2O_8Si_2W$: C 47.29, H 8.16, N 3.15; found C 47.40, H 8.31, N 2.98.

[PhC≡W(NHMe$_2$)(NMe$_2$)(OSiPh$_3$)$_2$], 16. A solution of triphenylsilanol (2.0 equiv., 238.7 mg, 863.6 μmol) in toluene (10 mL) was added slowly to a stirred solution of **4d** (175.0 mg, 431.8 μmol) in toluene (20 mL). After 3 h, the solvent was removed under reduced pressure, and the residue was dried in high vacuum to give a deep green solid in 91 % yield (358.9 mg, 393.1 μmol). **^{1}H NMR** (300.3 MHz, [D$_8$]toluene): δ = 2.13 (s, 3H; NH(CH_3)Me), 2.15 (s, 3H; NHMe(CH_3)), 2.29 (br s, 1H; N*H*Me$_2$), 2.75 (s, 3H; N(CH_3)Me), 3.90 (s, 3H; NMe(CH_3)), 6.73–6.83 (m, 3H; Ar-*H*), 7.13–7.21 (m, 20H; Ar-*H*), 7.82–7.91 (m, 12H; Ar-*H*); **^{13}C NMR** (75.5 MHz, [D$_8$]toluene): δ = 40.7 ($NHMe_2$), 42.7 (N(CH_3)Me), 59.8 (NMe(CH_3)), 127.4 (*Ph*C≡), 128.0 (Si*Ph*$_3$), 129.3 (*Ph*C≡), 129.6 (Si*Ph*$_3$), 131.7 (*Ph*C≡), 136.0 (Si*Ph*$_3$), 138.7 (Si*Ph*$_3$), 148.1 (*Ph*C≡), 275.9 (W≡*C*); **elemental analysis** calcd. (%) for $C_{47}H_{48}N_2O_2Si_2W$: C 61.84, H 5.30, N 3.07; found C 61.89, H 5.191, N 2.71.

[PhC≡W(NHMe$_2$){OC(CF$_3$)$_2$Me}{OSi(O-*t*-Bu)$_3$}$_2$], 17. A solution of Me(CF_3)$_2$COH (1.0 equiv., 134.8 mg, 0.740 mmol) in a small amount of *n*-pentane was added slowly to a solution of **15** (658.2 mg, 740.4 μmol) in *n*-pentane (30 mL). After stirring for 2 h at ambient temperature, the reaction mixture was concentrated under reduced pressure and stored at –35 °C. The product was isolated as orange crystals in 75 % yield (569.7 mg, 555.3 μmol). The crystals were suitable for X-ray diffraction analysis. **^{1}H NMR** (300.1 MHz, C_6D_6): δ = 1.45 (s, 54H; 6 × C(CH_3)), 2.03 (br m, 3H; OC(CF_3)$_2$CH_3), 2.78 (s, 3H; NH(CH_3)Me), 2.80 (s, 3H; NHMe(CH_3)), 5.61 (sept, $^3J_{H,H}$ = 5.8 Hz, 1H; N*H*Me$_2$), 6.70 (tt, $^3J_{H,H}$ = 7.4 Hz, $^4J_{H,H}$ = 1.4 Hz, 1H; *para-H*), 7.14–7.19 (m, 2H (overlapped with the solvent residual signal); Ar-C*H)*, 7.22–7.30 (m, 2H; Ar-C*H*); **^{13}C NMR** (75.5 MHz, C_6D_6): δ = 21.2 (OC(CF_3)$_2$CH_3), 31.9 (C(CH_3)$_3$), 42.2 ($NHMe_2$), 73.2 (*C*Me$_3$), 82.9 (m; O*C*(CF_3)$_2$CH$_3$), 124.9 (q, $^1J_{C,F}$ = 290 Hz; *C*F_3), 127.0 (Ar-*C*H), 127.3 (Ar-*C*H), 133.9 (Ar-*C*H), 145.4 (Ar-*C*$_q$), 281.3 (W≡*C*); **^{19}F NMR** (188.3 MHz, C_6D_6): δ = –76.2 (CF_3).

Synthesis of [PhC≡W(NHMe$_2$)(OSiPh$_3$)$_3$], 18. A solution of Ph_3SiOH (3.0 equiv., 1.023 g, 3.702 mmol) in toluene (10 mL) was added to a solution of **4d** (500 mg, 1.2340 mmol) in toluene (40 mL). The reaction mixture was stirred overnight at ambient temperature, and the solvent was removed under reduced pressure. The remaining residue was stirred for 20 min in *n*-pentane (20 mL), filtered, and then the collected solid was washed with *n*-pentane (3 × 5 mL) and dried under high vacuum to give a brownish-pink solid in 88 % yield (1.242 g, 1.085 mmol). Red single crystals were obtained from a concentrated dichloromethane solution at –35 °C. **^{1}H NMR** (300.1 MHz, C_6D_6): δ = 1.80 (s, 3H; NH(CH_3)Me), 1.82 (s, 3H; NHMe(CH_3)), 2.73 (sept, $^3J_{H,H}$ = 5.9 Hz, 1H; *H*NMe_2), 6.43–6.48 (m, 2H; Ar-*H*), 6.69 (tt, $^3J_{H,H}$ = 7.4 Hz, $^4J_{H,H}$ = 1.2 Hz, 1H; *para-H*), 6.87 (br t, 6H; Ar-*H*), 6.99–7.10 (m, 15H; Ar-*H*), 7.10–7.22 (m, 6H (overlapped with the solvent residual signal); Ar-*H*), 7.74–7.78 (m, 2H; Ar-*H*), 7.82–7.87 (m, 6H; Ar-*H*), 7.87–7.94 (m, 12H; Ar-*H*); **^{13}C NMR** (75.5 MHz, C_6D_6): δ = 42.3 ($NHMe_2$), 126.9 (*Ph*C≡), 127.9 (Si*Ph*$_3$), 128.1 (Si*Ph*$_3$), 128.2 (*Ph*C≡), 129.5 (Si*Ph*$_3$), 129.9 (Si*Ph*$_3$), 133.9 (*Ph*C≡), 136.2 (Si*Ph*$_3$), 136.4 (Si*Ph*$_3$), 137.4 (Si*Ph*$_3$), 137.7 (Si*Ph*$_3$), 145.9 (*Ph*C≡), 277.9 (W≡*C*); **elemental analysis** calcd. (%) for $C_{63}H_{57}NO_3Si_3W$: C 66.13, H 5.02, N 1.22; found C 65.75, H 4.96, N 1.21.

$[W_2(NMe_2)_4\{OC(CF_3)Me_2\}_2]$, 19a. A solution of 1,1,1-trifluoro-*tert*-butanol (2.0 equiv., 40.5 mg, 316.4 μmol) in toluene (2 mL) was added slowly to a solution of $[W_2(NMe_2)_6]$ (**3a**, 100 mg, 0.158 mmol) in toluene (10 mL). After stirring the reaction mixture for 8 h at ambient temperature, the solvent was removed under reduced pressure, and the remaining solid was sublimed at 120 °C and 10^{-3} mbar to give a yellow microcrystalline solid in 68 % yield (85.4 mg, 107.0 μmol). Single crystals were obtained from a concentrated *n*-pentane solution at –35 °C. **Elemental analysis** calcd. (%) for $C_{16}H_{36}F_6N_4O_2W_2$: C 24.08, H 4.55, N 7.02; found C 24.28, H 4.24, N 6.96.

$[W_2(NMe_2)_4\{OC(CF_3)_2Me\}_2]$, 19b. A solution of 1,1,1,3,3,3-hexafluoro-2-methylpropan-2-ol (2.0 equiv., 230 mg, 1.266 mmol) in toluene (5 mL) was added slowly to a solution of **3a** (400.0 mg, 632.8 μmol) in toluene (40 mL). After stirring the reaction mixture for 8 h at ambient temperature, the solvent was removed under reduced pressure, and the remaining solid was sublimed at 120 °C and 10^{-3} mbar to give a yellow microcrystalline solid in 70 % yield (401.4 mg, 443.0 μmol). Single crystals were obtained from a concentrated *n*-pentane solution at –35 °C. **^{1}H NMR** (600.1 MHz, C_6D_6): δ = 1.75 (m, 6H; 2 × C(CF$_3$)$_2$(C*H*$_3$), *meso*-1,2–**19b**), 1.78 (m, 3H; 2 × C(CF$_3$)$_2$(C*H*$_3$), *rac*-1,2–**19b**), 2.11–2.63 (br m, 12H + 6H; 4 × N(C*H*$_3$)Me, *meso*/*rac*-1,2–**19b**), 3.80–4.46 (br m, 12H + 6H; 4 × NMe(C*H*$_3$), *meso*/*rac*-1,2–**19b**); **^{13}C NMR** (150.9 MHz, C_6D_6): δ = 19.5 (C(CF$_3$)$_2$(*C*H$_3$)), 20.3 (C(CF$_3$)$_2$(*C*H$_3$)), 38.8 (NMe$_2$), 45.4 (NMe$_2$), 59.1 (NMe$_2$), 61.7 (NMe$_2$), 82.0 (m; O*C*(CF$_3$)Me), 124.6 (q, $^1J_{C,F}$ = 290 Hz; *C*F$_3$), 124.7(q, $^1J_{C,F}$ = 288 Hz; *C*F$_3$), 124.9 (q, $^1J_{C,F}$ = 288 Hz; *C*F$_3$); **^{19}F NMR** (376.8 MHz, C_6D_6): δ = –78.2 (q, $^4J_{F,F}$ = 9.4 Hz, 3F; 2 × *C*F$_3$, *rac*-1,2–**19b**), –78.6 (s, 12F; 4 × *C*F$_3$, *meso*-1,2–**19b**), –78.9 (q, $^4J_{F,F}$ = 9.4 Hz, 3F; 2 × *C*F$_3$, *rac*-1,2–**19b**), the isomeric mixture of *meso*-1,2–**19b** and *rac*-1,2–**19b** has a 2:1 ratio; **elemental analysis** calcd. (%) for $C_{16}H_{30}F_{12}N_4O_2W_2$: C 21.21, H 3.34, N 6.18; found C 21.08, H 3.14, N 5.72. Although the nitrogen content is not sufficiently accurate, it is provided to illustrate the best value obtained to date.

$[W_2(NMe_2)_4\{OC(CF_3)_3\}_2]$, 19c. A solution of perfluoro-*tert*-butanol (2.0 equiv., 97 mg, 0.411 mmol) in toluene (2 mL) was added slowly to a solution of **3a** (130.0 mg, 0.206 mmol) in toluene (10 mL). After stirring the reaction mixture for 8 h at ambient temperature, the solvent was removed under reduced pressure, and the remaining solid was sublimed at 120 °C and 10^{-3} mbar to give an orange solid in 70 % yield (146 mg, 0.144 mmol). Single crystals were obtained from a concentrated *n*-pentane solution at –35 °C. **Elemental analysis** calcd. (%) for $C_{16}H_{24}F_{18}N_4O_2W_2$: C 18.95, H 2.39, N 5.53; found C 19.15, H 2.51, N 5.54.

Standard procedure for the self-metathesis of 5-benzyloxy-2-pentyne. In an argon-filled glovebox, a 5 mL flask was charged with powdered molecular sieves 5 Å (250 mg), *n*-decane (0.05 mL), 5-benzyloxy-2-pentyne (0.25 mmol), and toluene (1.5 mL). A sample (0.05 mL) was then taken for the GC reference. After addition of the catalyst (**14**–**18**, 1 mol-%, 2.5 μmol; **19**, 0.5 mol-%, 1.25 μmol), 0.05 mL aliquots were collected at defined time intervals (1, 2, 3, 4, 5, 10, 20, 30, 60, 120, and 180 min). Additional aliquots were collected every 30 min (the final sample after 600 min) for complexes **19**. All samples were filtered directly through neutral alox and rinsed three times with diethyl ether. The filtrate was analyzed via GC, and the crude reaction mixtures at the end of the metathesis reactions were analyzed via GPC (see pp S35–S39).

Supporting Information (see footnote on the first page of this article): Additional experimental details, including solid-state structure determinations, NMR spectra and GPC traces.

Conflict of Interest

The authors declare no competing financial interest.

Acknowledgments

We thank to Dr. Dirk Bockfeld for determination of the X-ray crystal structure of *meso*-1,2-**19c**. Financial support by the Deutsche Forschungsgemeinschaft (DFG) through grant Ta 189/12-1 is gratefully acknowledged. Open access funding enabled and organized by Projekt DEAL.

Keywords: Alkylidyne complexes · Alkyne metathesis · Metal–metal triple bonds · Tungsten · Homogeneous catalysis

[1] F. Pennella, R. L. Banks, G. C. Bailey, *Chem. Commun.* **1968**, 1548–1549.
[2] a) A. Fürstner, P. W. Davies, *Chem. Commun.* **2005**, 2307–2320; b) A. Mortreux, O. Coutelier, *J. Mol. Catal. A* **2006**, *254*, 96–104; c) W. Zhang, J. S. Moore, *Adv. Synth. Catal.* **2007**, *349*, 93–120; d) M. Tamm, X. Wu, *Chem. Today* **2010**, *28*, 60–63; e) X. Wu, M. Tamm, *Beilstein J. Org. Chem.* **2011**, *7*, 82–93; f) A. Fürstner, *Angew. Chem. Int. Ed.* **2013**, *52*, 2794–2819; *Angew. Chem.* **2013**, *125*, 2860; g) C. Deraedt, M. d'Halluin, D. Astruc, *Eur. J. Inorg. Chem.* **2013**, *2013*, 4881–4908; h) R. R. Schrock, *Chem. Commun.* **2013**, *49*, 5529–5531; i) H. Yang, Y. Jin, Y. Du, W. Zhang, *J. Mater. Chem. A* **2014**, *2*, 5986–5993; j) H. Ehrhorn, M. Tamm, *Chem. Eur. J.* **2019**, *25*, 3190–3208; k) D. Lee, I. Volchkov, S. Y. Yun, *Alkyne Metathesis.* In *Organic Reactions, Vol. 102* (Ed.: P. A. Evans), John Wiley & Sons, Hoboken, NJ (USA), **2020**, p. 613–931.
[3] a) R. R. Schrock, J. Sancho, S. F. Pederson, S. C. Virgil, R. H. Grubbs, *2,2-Dimethylpropylidyne Tungsten(VI) Complexes and Precursors for their Syntheses.* In *Inorganic Syntheses, Vol. 26* (Ed.: H. D. Kaesz), John Wiley & Sons, Hoboken, NJ (USA), **1989**, p. 44–51; b) J. H. Freudenberger, R. R. Schrock, M. R. Churchill, A. L. Rheingold, J. W. Ziller, *Organometallics* **1984**, *3*, 1563–1573.
[4] J. H. Freudenberger, R. R. Schrock, *Organometallics* **1986**, *5*, 1411–1417.
[5] a) A. Mayr, G. A. McDermott, *J. Am. Chem. Soc.* **1986**, *108*, 548–549; b) G. A. McDermott, A. M. Dorries, A. Mayr, *Organometallics* **1987**, *6*, 925–931; c) B. Haberlag, X. Wu, K. Brandhorst, J. Grunenberg, C. G. Daniliuc, P. G. Jones, M. Tamm, *Chem. Eur. J.* **2010**, *16*, 8868–8877.
[6] a) R. R. Schrock, M. L. Listemann, L. G. Sturgeoff, *J. Am. Chem. Soc.* **1982**, *104*, 4291–4293; b) R. R. Schrock, *Science* **1983**, *219*, 13–18; c) M. L. Listemann, R. R. Schrock, *Organometallics* **1985**, *4*, 74–83; d) R. R. Schrock, *Acc. Chem. Res.* **1986**, *19*, 342–348; e) I. A. Latham, L. R. Sita, R. R. Schrock, *Organometallics* **1986**, *5*, 1508–1510; f) T. A. Budzichowski, M. H. Chisholm, D. B. Tiedtke, N. E. Gruhn, D. L. Lichtenberger, *Polyhedron* **1998**, *17*, 705–711; g) M. H. Chisholm, *Chem. Rec.* **2001**, *1*, 12–23; h) H. Ehrhorn, J. Schlösser, D. Bockfeld, M. Tamm, *Beilstein J. Org. Chem.* **2018**, *14*, 2425–2434.
[7] a) F. A. Cotton, B. R. Stults, J. M. Troup, M. H. Chisholm, M. W. Extine, *J. Am. Chem. Soc.* **1975**, *97*, 1242–1243; b) M. H. Chisholm, F. A. Cotton, M. W. Extine, B. R. Stults, *J. Am. Chem. Soc.* **1976**, *98*, 4477–4485; c) M. Akiyama, M. H. Chisholm, F. A. Cotton, M. W. Extine, D. A. Haitko, D. Little, P. E. Fanwick, *Inorg. Chem.* **1979**, *18*, 2266–2270; d) M. H. Chisholm, D. A. Haitko, C. A. Murillo, F. A. Cotton, S. Han, *12. Syntheses of Dimethylamido Compounds Containing Metal-to-Metal Triple Bonds Between Molybdenum and Tungsten Atoms.* In *Inorganic Syntheses, Vol. 21* (Ed.: J. P. Fackler, Jr.), John Wiley & Sons, New York, NY (USA), **1982**, p. 51–57.
[8] Also other reducing agents, such as antimony, mercury, $[W(CO)_6]$, or red phosphorus, have been employed; see: a) V. Kolesnichenko, D. C. Swenson, L. W. Messerle, *Inorg. Chem.* **1998**, *37*, 3257–3262; b) M. H. Chisholm, M. W. Extine, *J. Am. Chem. Soc.* **1975**, *97*, 5625–5627.
[9] M. H. Chisholm, C. B. Hollandsworth, *$X_3M{\equiv}MX_3$ Compounds of Molybdenum and Tungsten*. In *Multiple Bonds Between Metal Atoms*, 3rd ed. (Eds.: F. A. Cotton, C. A. Murillo, R. A. Walton), Springer US, Boston, MA, **2005**, p. 203–250.

[10] R. R. Schrock, D. N. Clark, J. Sancho, J. H. Wengrovius, S. M. Rocklage, S. F. Pedersen, *Organometallics* **1982**, *1*, 1645–1651.
[11] I. Feinstein-Jaffe, J. C. Dewan, R. R. Schrock, *Organometallics* **1985**, *4*, 1189–1193.
[12] K. R. McClain, C. T. O'Donohue, Z. Shi, A. V. Walker, K. A. Abboud, T. J. Anderson, L. McElwee-White, *Eur. J. Inorg. Chem.* **2012**, *2012*, 4579–4584.
[13] a) Y.-C. Tsai, P. L. Diaconescu, C. C. Cummins, *Organometallics* **2000**, *19*, 5260–5262; b) J. M. Blackwell, J. S. Figueroa, F. H. Stephens, C. C. Cummins, *Organometallics* **2003**, *22*, 3351–3353; c) W. Zhang, S. Kraft, J. S. Moore, *J. Am. Chem. Soc.* **2004**, *126*, 329–335; d) W. Zhang, Y. Lu, J. S. Moore, G. Seidel, A. Fürstner, *Org. Synth.* **2007**, *84*, 163–176; e) K. Jyothish, W. Zhang, *Angew. Chem. Int. Ed.* **2011**, *50*, 3435–3438; *Angew. Chem.* **2011**, *123*, 3497; f) K. Jyothish, Q. Wang, W. Zhang, *Adv. Synth. Catal.* **2012**, *354*, 2073–2078; g) H. Yang, Z. Liu, W. Zhang, *Adv. Synth. Catal.* **2013**, *355*, 885–890; h) D. W. Paley, D. F. Sedbrook, J. Decatur, F. R. Fischer, M. L. Steigerwald, C. Nuckolls, *Angew. Chem. Int. Ed.* **2013**, *52*, 4591–4594; *Angew. Chem.* **2013**, *125*, 4689; i) M. Ortiz, C. Yu, Y. Jin, W. Zhang, *Top. Curr. Chem.* **2017**, *375*, No. 69.
[14] a) K. R. McClain, C. T. O'Donohue, A. Koley, R. O. Bonsu, K. A. Abboud, J. C. Revelli, T. J. Anderson, L. McElwee-White, *J. Am. Chem. Soc.* **2014**, *136*, 1650–1662; b) A. Koley, C. T. O'Donohue, M. M. Nolan, K. R. McClain, R. O. Bonsu, R. Y. Korotkov, T. J. Anderson, L. McElwee-White, *Chem. Mater.* **2015**, *27*, 8326–8336.
[15] a) S. Beer, C. G. Hrib, P. G. Jones, K. Brandhorst, J. Grunenberg, M. Tamm, *Angew. Chem. Int. Ed.* **2007**, *46*, 8890–8894; *Angew. Chem.* **2007**, *119*, 9047; b) S. Beer, K. Brandhorst, J. Grunenberg, C. G. Hrib, P. G. Jones, M. Tamm, *Org. Lett.* **2008**, *10*, 981–984; c) S. Beer, K. Brandhorst, C. G. Hrib, X. Wu, B. Haberlag, J. Grunenberg, P. G. Jones, M. Tamm, *Organometallics* **2009**, *28*, 1534–1545; d) S. Lysenko, B. Haberlag, X. Wu, M. Tamm, *Macromol. Symp.* **2010**, *293*, 20–23; e) X. Wu, C. G. Daniliuc, C. G. Hrib, M. Tamm, *J. Organomet. Chem.* **2011**, *696*, 4147–4151; f) S. Lysenko, C. G. Daniliuc, P. G. Jones, M. Tamm, *J. Organomet. Chem.* **2013**, *744*, 7–14; g) X. Wu, M. Tamm, *Coord. Chem. Rev.* **2014**, *260*, 116–138; h) B. Haberlag, M. Freytag, P. G. Jones, M. Tamm, *Adv. Synth. Catal.* **2014**, *356*, 1255–1265.
[16] a) S. Lysenko, B. Haberlag, C. G. Daniliuc, P. G. Jones, M. Tamm, *ChemCatChem* **2011**, *3*, 115–118; b) S. Lysenko, J. Volbeda, P. G. Jones, M. Tamm, *Angew. Chem. Int. Ed.* **2012**, *51*, 6757–6761; *Angew. Chem.* **2012**, *124*, 6861; c) S. T. Li, T. M. Schnabel, S. Lysenko, K. Brandhorst, M. Tamm, *Chem. Commun.* **2013**, *49*, 7189–7191; d) T. M. Schnabel, D. Melcher, K. Brandhorst, D. Bockfeld, M. Tamm, *Chem. Eur. J.* **2018**, *24*, 9022–9032.
[17] C. Bittner, H. Ehrhorn, D. Bockfeld, K. Brandhorst, M. Tamm, *Organometallics* **2017**, *36*, 3398–3406.
[18] a) B. Haberlag, M. Freytag, C. G. Daniliuc, P. G. Jones, M. Tamm, *Angew. Chem. Int. Ed.* **2012**, *51*, 13019–13022; *Angew. Chem.* **2012**, *124*, 13195; b) D. P. Estes, C. Bittner, Ò. Àrias, M. Casey, A. Fedorov, M. Tamm, C. Copéret, *Angew. Chem. Int. Ed.* **2016**, *55*, 13960–13964; *Angew. Chem.* **2016**, *128*, 14166; c) D. P. Estes, C. P. Gordon, A. Fedorov, W.-C. Liao, H. Ehrhorn, C. Bittner, M. L. Zier, D. Bockfeld, K. W. Chan, O. Eisenstein, C. Raynaud, M. Tamm, C. Copéret, *J. Am. Chem. Soc.* **2017**, *139*, 17597–17607.
[19] a) S. W. von Kugelgen, D. E. Bellone, R. R. Cloke, W. S. Perkins, F. R. Fischer, *J. Am. Chem. Soc.* **2016**, *138*, 6234–6239; b) S. W. von Kugelgen, R. Sifri, D. E. Bellone, F. R. Fischer, *J. Am. Chem. Soc.* **2017**, *139*, 7577–7585; c) H. Jeong, S. W. von Kugelgen, D. E. Bellone, F. R. Fischer, *J. Am. Chem. Soc.* **2017**, *139*, 15509–15514; d) Ò. Àrias, H. Ehrhorn, J. Härdter, P. G. Jones, M. Tamm, *Organometallics* **2018**, *37*, 4784–4800.
[20] a) M. Koy, I. Elser, J. Meisner, W. Frey, K. Wurst, J. Kästner, M. R. Buchmeiser, *Chem. Eur. J.* **2017**, *23*, 15484–15490; b) I. Elser, J. Groos, P. M. Hauser, M. Koy, M. van der Ende, D. Wang, W. Frey, K. Wurst, J. Meisner, F. Ziegler, J. Kästner, M. R. Buchmeiser, *Organometallics* **2019**, *38*, 4133–4146; c) P. M. Hauser, M. van der Ende, J. Groos, W. Frey, D. Wang, M. R. Buchmeiser, *Eur. J. Inorg. Chem.* **2020**, *2020*, 3070–3082.
[21] J. Heppekausen, R. Stade, R. Goddard, A. Fürstner, *J. Am. Chem. Soc.* **2010**, *132*, 11045–11057.
[22] a) P. Persich, J. Llaveria, R. Lhermet, T. de Haro, R. Stade, A. Kondoh, A. Fürstner, *Chem. Eur. J.* **2013**, *19*, 13047–13058; b) A. Fürstner, *Alkyne Metathesis in Organic Synthesis*. In *Modern Alkyne Chemistry* (Eds.: B. M. Trost, C.-J. Li), Wiley-VCH Verlag GmbH & Co. KGaA, Weinheim (Germany), **2015**, p. 69–112.
[23] F. Ungeheuer, A. Fürstner, *Chem. Eur. J.* **2015**, *21*, 11387–11392.
[24] a) J. H. Wengrovius, J. Sancho, R. R. Schrock, *J. Am. Chem. Soc.* **1981**, *103*, 3932–3934; b) F. A. Cotton, W. Schwotzer, E. S. Shamshoum, *J. Organomet. Chem.* **1985**, *296*, 55–68.
[25] L. Yang, D. R. Powell, R. P. Houser, *Dalton Trans.* **2007**, 955–964.
[26] A. G. Orpen, L. Brammer, F. H. Allen, O. Kennard, D. G. Watson, R. Taylor, *J. Chem. Soc., Dalton Trans.* **1989**, S1–S83.
[27] a) M. Bindl, R. Stade, E. K. Heilmann, A. Picot, R. Goddard, A. Fürstner, *J. Am. Chem. Soc.* **2009**, *131*, 9468–9470; b) J. Heppekausen, R. Stade, A. Kondoh, G. Seidel, R. Goddard, A. Fürstner, *Chem. Eur. J.* **2012**, *18*, 10281–10299; c) R. Lhermet, A. Fürstner, *Chem. Eur. J.* **2014**, *20*, 13188–13193.
[28] A. W. Addison, T. N. Rao, J. Reedijk, J. van Rijn, G. C. Verschoor, *J. Chem. Soc., Dalton Trans.* **1984**, 1349–1356.
[29] A. D. Lackner, A. Fürstner, *Angew. Chem. Int. Ed.* **2015**, *54*, 12814–12818; *Angew. Chem.* **2015**, *127*, 13005.
[30] a) T. W. Coffindaffer, I. P. Rothwell, J. C. Huffman, *Inorg. Chem.* **1985**, *24*, 1643–1646; b) T. W. Coffindaffer, G. P. Niccolai, D. Powell, I. P. Rothwell, *J. Am. Chem. Soc.* **1985**, *107*, 3572–3583; c) T. A. Budzichowski, M. H. Chisholm, D. B. Tiedtke, J. C. Huffman, W. E. Streib, *Organometallics* **1995**, *14*, 2318–2324.
[31] P. Pyykkö, S. Riedel, M. Patzschke, *Chem. Eur. J.* **2005**, *11*, 3511–3520.
[32] X. Wu, *New Tungsten Alkylidyne Complexes as Catalysts for Alkyne Metathesis*, PhD Thesis, TU Braunschweig; Verlag Dr. Hut, Braunschweig (Germany), **2011**.
[33] W. L. F. Armarego, C. L. L. Chai, *Purification of Laboratory Chemicals*, 6th ed.; Butterworth-Heinemann, Amsterdam (Netherlands), **2008**.
[34] D. C. Bradley, I. M. Thomas, *J. Chem. Soc.* **1960**, 3857–3861.
[35] G. M. Sheldrick, *Acta Crystallogr., Sect. A: Found. Crystallogr.* **2008**, *64*, 112–122.
[36] G. M. Sheldrick, *Acta Crystallogr., Sect. C: Struct. Chem.* **2015**, *71*, 3–8.
[37] Siemens. *XP. Molecular Graphics Program, Version 5.03*; Siemens Analytical X-ray Instruments Inc., Madison (WI, USA), **2004**.

Received: September 3, 2019

Full Paper
doi.org/10.1002/ejic.202000835

Alkyne Metathesis

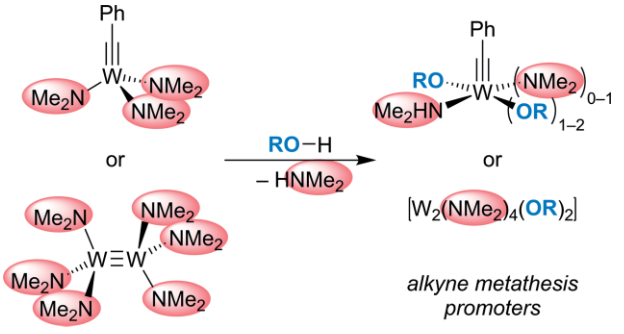

Mixed ligand systems for alkyne metathesis. Tungsten alkyne metathesis catalysts bearing a combination of alkoxide and amide ligands were readily synthesized via partial alcoholysis of tris(dimethylamido)tungsten precursors such as [PhC≡W(NMe_2)$_3$] and [W_2(NMe_2)$_6$].

doi.org/10.1002/ejic.202000835